Proceeding of International Joint Conference on UNESA
Homepage : https://proceeding.unesa.ac.id/index.php/pijcu
e-ISSN : 3032-3762

PIJCU, Vol. 3, No. 1, December 2025
Page 1-10

Integrated VSD-PLC-HMI Based Speed Control System For Three-Phase Induction Motor In Vertical Drive Applications

Harrij Mukti K[1*], Rohmanita Duanaputri[2], Rachmat Sutjipto[3], Dhimas Dhesah K[4], M. Fahmi Hakim[5]
[1*,2,3,4,5] State Polytechnic of Malang, Malang, Indonesia

Keywords:
Induction Motor
PWM Inverter
HMI (Human Machine Interface)
Speed Control

ABSTRACT

This study presents the design and implementation of a speed regulation system for a three-phase induction motor using a Variable Speed Drive (VSD) integrated with a Programmable Logic Controller (PLC) and Human Machine Interface (HMI). The system was developed to address the limitations of previous studies, which focused primarily on soft starting or braking functions without real-time control integration. The proposed system enables soft starting, precise speed regulation, and voltage control through real-time frequency adjustments. Under experimental testing, the motor achieved a stable speed of 1500 RPM at 50 Hz, with startup current limited to 0.94 A under no-load and 1.3 A under load conditions. Voltage output was consistently linear, reaching up to 381 V (no-load) and 369 V (with load), indicating reliable performance across the frequency range. Compared to earlier works, this system demonstrates improved integration and feedback responsiveness, making it suitable for industrial applications that require efficient and adaptive motor control.

INTRODUCTION

Three-phase induction motors are widely used in industry due to their high durability and simple structure. However, these motors generate large starting currents, about 5-7 times the nominal current (Hardi et al., 2022), which can cause significant voltage drops and degrade the quality of electric power (Siregar et al., 2025) such as mechanical pounding (Patil & Porate, 2009). To solve this problem, speed regulation through frequency shifting is considered to be the most efficient and flexible method (Taru et al., n.d.).

Inverters are used in this system with the working principle of converting AC voltage into DC, then back into AC with an adjustable frequency (Singarimbun & Anisah, n.d.). The integration of inverters with PLCs and HMIs further enhances the flexibility and efficiency of the system, as it enables automatic settings and real-time monitoring of parameters via digital displays (Suji Prasad et al., 2019) This system is proven to provide more accurate speed regulation than conventional methods (Gawade et al., 2019). In addition, the Human Machine Interface (HMI) allows the operator to monitor and adjust the motor speed directly and intuitively (Yuhendri et al., 2025).

Meanwhile, the use of Arduino Uno-based soft starters has also proven effective in reducing inrush current during the starting process (Mukti et al., 2025). However, previous research still focuses on reducing current without highlighting speed stability or braking systems. In fact, in industrial applications such as traditional oil mining, a fast-braking system is very important (Mukti et al., 2024). However, prior studies primarily emphasize current reduction or basic speed control, lacking a comprehensive solution that integrates soft-start, precise speed regulation, and braking functionality for heavy-

duty applications such as oil drilling. This research addresses this gap by designing a unified control system using VSD, PLC, and HMI, ensuring efficient and safe motor operations across varied industrial scenarios.

RESEARCH METHOD

The research methodology used in this study is illustrated in the flowchart shown in **Figure 1**. The flowchart outlines the specific stages carried out in the development of a VSD-based control system for a three-phase induction motor, starting from system specification, hardware-software integration, to performance testing. Unlike standard procedures that emphasize only hardware development, this research highlights integrated control logic, HMI interface design, and comparative evaluation with previous works.

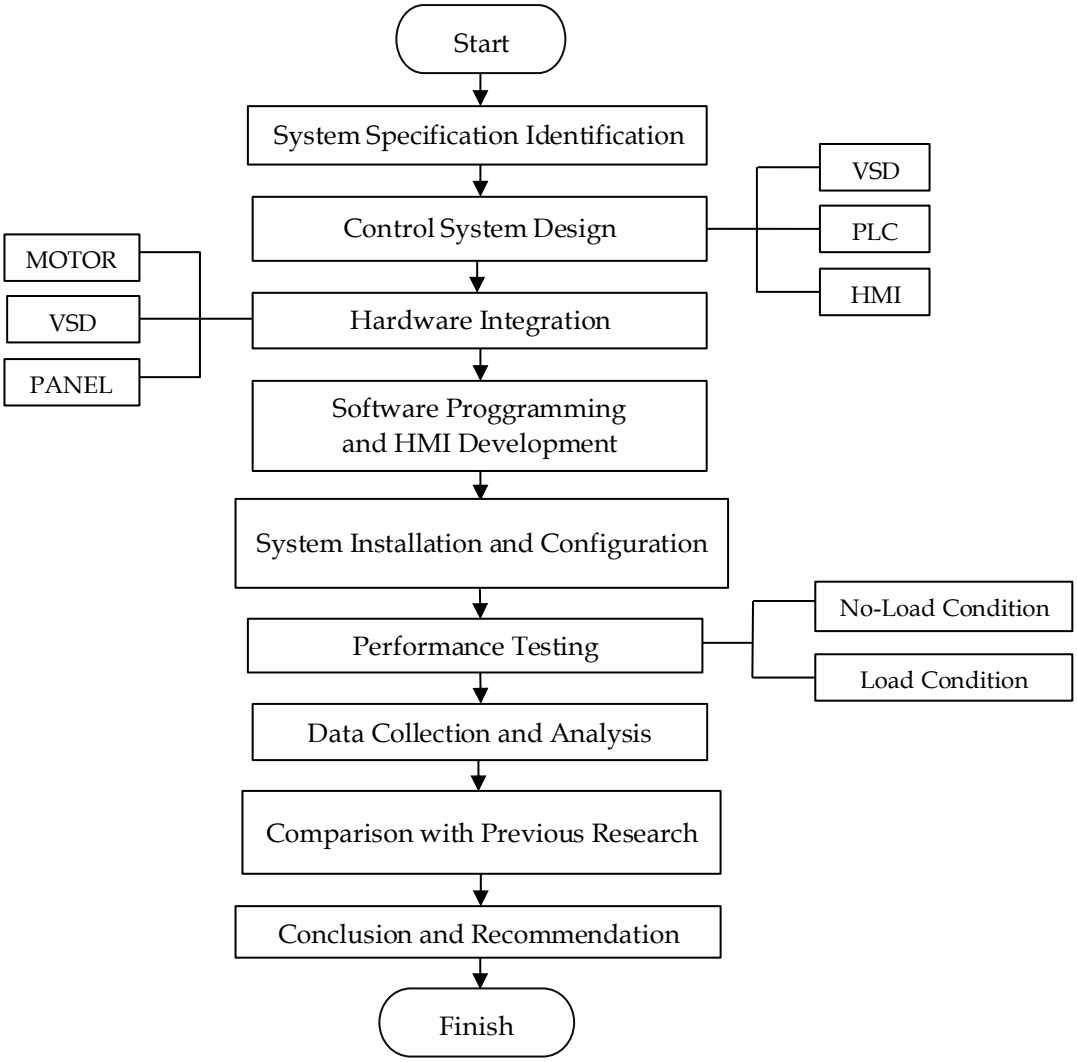

Figure 1. Research Flow Chart

1. Hardware Design

The hardware design includes the power supply setup, panel box modification, motor speed control, and inverter wiring. It begins with selecting an induction motor, SHZK-type VSD, PLC, HMI, and supporting components. The VSD parameters are adjusted based on the motor's nameplate data (voltage, power, frequency, and speed). Operated via PLC digital input, this setup enables flexible speed control. Cable connections are configured according to each terminal's function to ensure optimal operation. Figure 2 shows the main wiring diagram linking the VSD, PLC, HMI, and motor for frequency-based speed regulation.

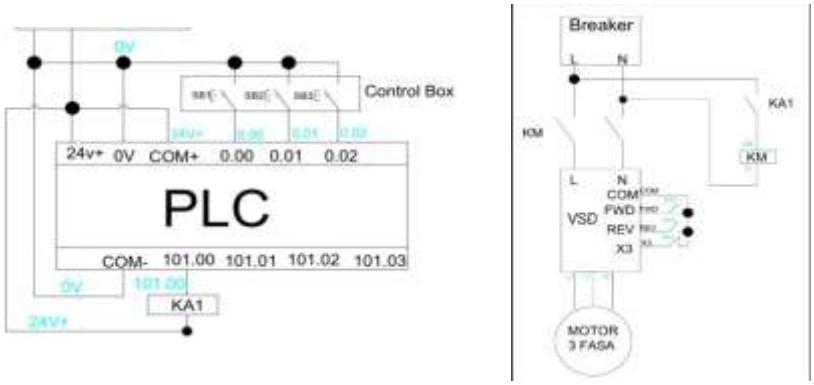

Figure 2. Speed Regulation Control and Power Circuit

This speed control circuit is used in the prototype with the VSD as the speed regulator through frequency shifting, and the HMI-PLC as the main control unit. The system requires a 24 VDC power supply to operate the PLC and HMI and activate the 24 VDC relays that control the contactors to the VSD. Commands from the HMI to the VSD are sent via Ethernet cable, while the VSD output is channeled to a three-phase induction motor as a load.

Figure 3 displays the complete arrangement of the control system hardware. This includes the mounted VSD, PLC controller, HMI panel, power supply, and the three-phase induction motor used during testing.

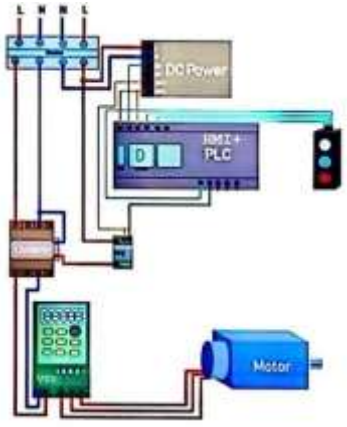

Figure 3. Overall, Tool Set

2. Software Design

The design of this system is done through several stages. The first stage is the preparation of devices, namely HMI + PLC Kinco type MK and SHZK VSD, as well as connecting NYAF cables and Ethernet cables for connection to laptops. The second stage is setting the parameters on the VSD to synchronize with the output of the PLC. The interface design and control logic of the software system are shown in **Figure 4**. This includes the PLC programming stages and the HMI visualization developed using KincoBuilder software.

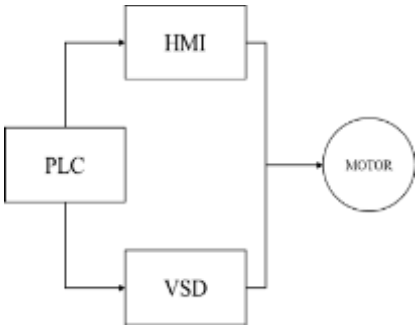

Figure 4. Software Design

3. Functional Blocks of the System

The overall control structure of the system is outlined in **Figure 5**, which presents the functional blocks and signal flow between the controller, inverter, and the three-phase motor. This structure enables automatic speed control based on real-time input from the HMI.

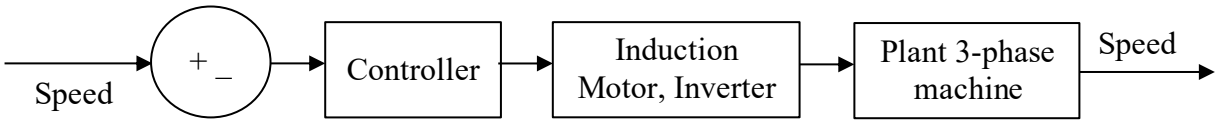

Figure 5. Functional Blocks of the System

Based on the picture, the system consists of several functional blocks, namely:

a. Cntroller (PLC): Functioning to regulate the work of the VSD according to commands from the HMI.
b. VSD (Variable Speed Drive): Controls the speed of a three-phase induction motor by changing the output frequency.
c. 3-Phase Induction Motor: As the main actuator whose speed is controlled by the VSD.
d. HMI (Human Machine Interface): Displaying motor speed and frequency parameters through the LCD screen, as well as control input to the system.

The working principle of this tool starts from the connection between software and hardware. Once connected, the system receives a frequency input of 0-60 Hz. The PLC, through the ladder diagram, sends commands to the expansion PLC to generate variable voltage using move and multiply instructions. This frequency value is converted into a voltage that is passed to the VSD. If there is a difference between the input value and the display on the VSD, the system performs automatic correction using compare logic until the values match.

RESULTS AND DISCUSSION

This chapter discusses the results of measurements and analysis of the system that has been designed. Testing is carried out on hardware and software as a whole to ensure that all components function properly, so that the system can run optimally.

1. Current Measurement Results and Analysis

The relationship between frequency and current under no-load conditions is illustrated in **Figure 6**. It provides insight into the current draw of the motor when operated without any mechanical load across a range of frequencies.

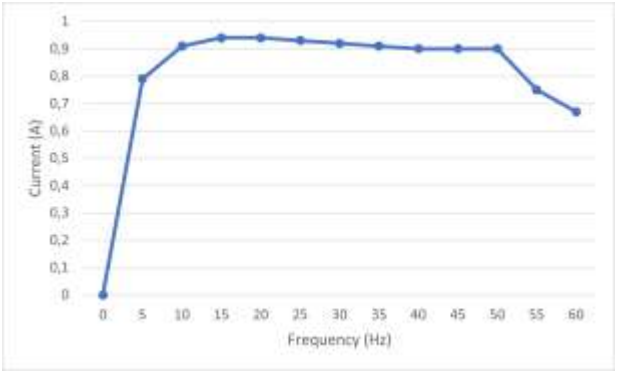

Figure 6. No-load current graph using VSD

Based on the no-load current graph using the VSD, it can be seen that the current increases significantly at the beginning of operation, especially between frequencies of 0 to 5 Hz, from almost 0 A to about 0.8 A. This increase occurs because the VSD starts to deliver current to rotate the motor from a standstill condition. In the frequency range of 10 to 20 Hz, the current reaches a peak value of about 0.94 A, which indicates that the motor starts to work stably even without load. Furthermore, at frequencies between 20 and 50 Hz, the current is relatively stable with a slight decrease, being in the range of 0.9 A, which indicates that the motor rotates smoothly and efficiently. However, when the frequency exceeds 50 Hz until it approaches 60 Hz, the current again decreases to around 0.7 A. This decrease occurs because the load is not present, so the VSD adjusts the current according to the minimum requirements of the motor. Overall, this graph shows that the VSD system is able to regulate the motor current well under no-load conditions, with an efficient and stable working pattern.

Figure 7 shows the current characteristics of the motor when operating under load. It reveals the VSD's ability to manage inrush current and maintain current stability during operation.

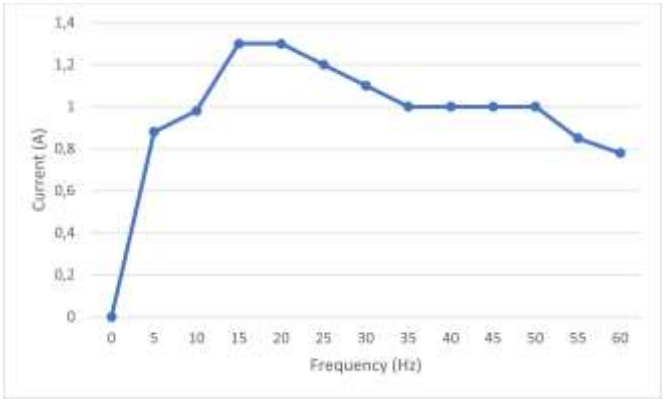

Figure 7. Current graph with load using VSD

Based on the graph of current with load using the VSD, it can be seen that the current increases significantly at the beginning of operation, especially between frequencies of 0 to 5 Hz, from almost 0 A to about 0.9 A. This increase occurs because the VSD starts to deliver current to rotate the motor from a standstill condition with the existing load. In the frequency range of 5 to 15 Hz, the current reaches a peak value of about 1.3 A, which indicates that the motor starts to work stably even with a load. Furthermore, at frequencies between 15 and 50 Hz, the current is relatively stable with little fluctuation, being in the range of 1.0 A, which indicates that the motor rotates efficiently under load conditions. However, when the frequency exceeds 50 Hz to near 60 Hz, the current again decreases to about 0.8 A. This decrease may occur because the VSD adjusts the current according to the minimum requirement of the motor under lower load conditions. Overall, this graph shows that the VSD system is able to regulate the motor current well under load conditions, with an efficient and stable working pattern, reflecting the VSD's ability to optimize motor performance at various frequencies. Speed Measurement Results and Analysis

2. Speed Measurement Result and Analysis

The motor's speed response at varying frequencies without load is depicted in **Figure 8**. This graph validates the proportional relationship between frequency and speed under no-load conditions.

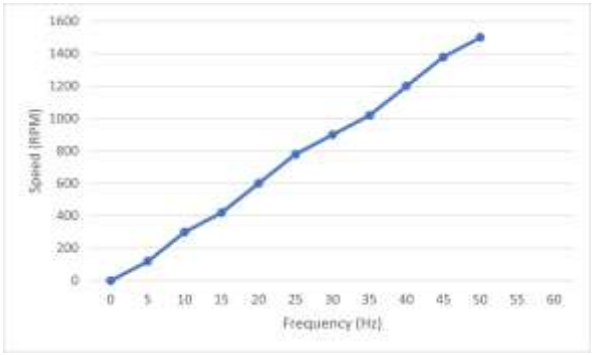

Figure 8. No-load speed graph using VSD

Based on the no-load speed graph using the VSD, it can be seen that the motor speed increases consistently as the frequency increases, starting from almost 0 RPM at a frequency of 0 Hz until it reaches about 1500 RPM at a frequency of 50 Hz. This steady increase indicates that any increase in frequency results in a proportional increase in speed, reflecting the efficiency of the VSD in regulating the motor speed. During this frequency range, the motor operates well in the absence of load, showing optimal performance. This graph confirms that the VSD system can effectively regulate the motor speed under no-load conditions, providing precise and stable control, which is very important in industrial applications where accurate speed regulation is required.

Figure 9 shows the speed of the motor when subjected to a mechanical load. The trend demonstrates how the system maintains speed stability across increasing frequency levels.

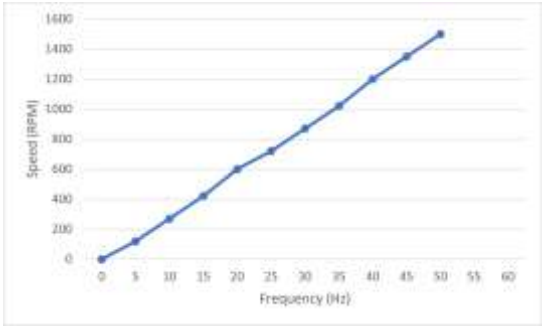

Figure 9. Speed graph with load using VSD

Based on the speed graph with load using VSD, it can be seen that the motor speed also increases consistently as the frequency increases. The motor speed starts from almost 0 RPM at a frequency of 0 Hz and reaches about 1500 RPM at a frequency of 50 Hz. This steady increase shows that despite the load, any increase in frequency still results in a proportional increase in speed, reflecting the ability of the VSD to efficiently manage the motor speed. Under load, the motor performs well, continuing to operate steadily without significant fluctuations in speed. This graph confirms that the VSD system is able to effectively manage the motor speed under load, providing precise and stable control. This is particularly important in industrial applications that require accurate speed regulation even under load conditions, demonstrating that VSDs can be relied upon to improve operational efficiency.

3. Voltage Measurement Results and Analysis

The voltage profile under no-load conditions is presented in **Figure 10**. It illustrates the linear voltage increase as the frequency rises, confirming the system's voltage regulation capability without significant fluctuations.

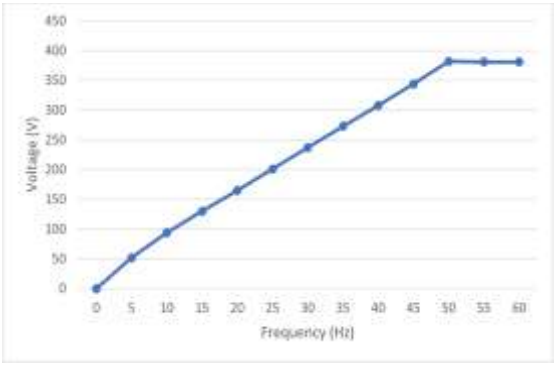

Figure 10. No-load voltage graph using VSD

Based on the no-load voltage graph using the VSD, it can be seen that the voltage increases consistently as the frequency increases. The voltage starts from almost 0 V at a frequency of 0 Hz and reaches about 381 V at a frequency of 50-60 Hz. This steady increase in voltage shows that the VSD effectively regulates the voltage for the motor as the frequency increases to ensure the motor can operate efficiently. During this frequency range, there is no significant fluctuation in the voltage, reflecting the good performance of the VSD system under no-load conditions. This graph confirms that the VSD system is able to provide precise and stable voltage to the motor under no-load conditions, which is a key factor for maintaining optimal motor performance. This shows that VSDs can reliably regulate voltage accurately, supporting operational efficiency in industrial applications.

Figure 11 illustrates the voltage behavior of the motor when under load. The voltage increases steadily with frequency, highlighting the reliability of the VSD in maintaining voltage consistency during loaded operation.

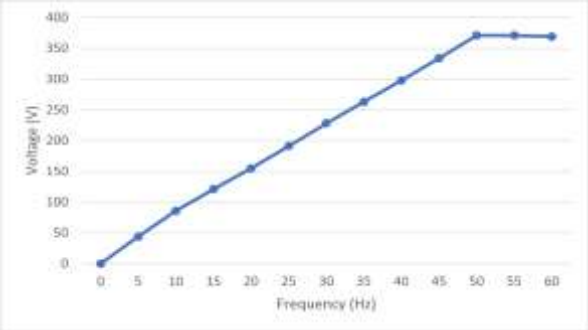

Figure 11. Voltage graph with load using VSD

Based on the graph of voltage versus frequency under load conditions using VSD, it can be seen that the voltage increases consistently as the frequency increases. The voltage starts from almost 0 V at a frequency of 0 Hz and reaches about 369 V at a frequency of 50 - 60 Hz. This steady increase in voltage shows that the VSD effectively regulates the voltage for the motor even under load conditions to ensure the motor operates optimally. Over this frequency range, the graph shows a strong linear relationship, with no significant fluctuations in the voltage, reflecting the good performance of the VSD system. This graph confirms that the VSD system is able to provide precise and stable

voltage to the motor under load conditions, which is a key factor for maintaining optimal motor performance. This shows that the VSD can reliably regulate the voltage accurately, supporting onal operating efficiency in various industrial applications despite the load.

CONCLUSION

Based on the tests carried out, the VSD-based motor control system integrated with PLC and HMI has been proven to effectively regulate motor performance under both no-load and load conditions. During startup, the system successfully limited the inrush current to approximately 0.94 A (no-load) and 1.3 A (with load), significantly lower than conventional direct-on-line methods. The motor speed increased proportionally with frequency, reaching up to 1500 RPM at 50 Hz, showing stable and accurate control. The voltage output was also linear, ranging from 0 V to 381 V (no-load) and 369 V (load) without significant fluctuations, indicating precise voltage regulation by the VSD.

Compared to previous studies such as (Mukti et al., 2025) which focused solely on soft starting, and (Mukti et al., 2024) which emphasized braking systems, this study provides a more comprehensive solution by integrating soft starting, speed control, and voltage monitoring into a unified system. The results also support the findings of (Gawade et al., 2019), but enhance them by incorporating real-time feedback via HMI for more responsive control.

For future research, it is recommended to develop the system further by integrating an intelligent braking mechanism and expanding remote monitoring capabilities via IoT-based platforms. This will enable broader industrial application and improve safety, responsiveness, and energy efficiency in real-time motor operations.

ACKNOWLEDGEMENTS

This research is supported by State Polytechnic of Malang.

REFERENCES

Gawade, O., Utekar, O., Ranjane, S., Raut, A., Sonune, R., & Mumbai, N. (2019). V/F Speed Control Technique of Three Phase Induction Motor. *International Journal of Innovative Research in Electrical, Electronics, Instrumentation and Control Engineering*, *7*(1), 2321–5526. https://doi.org/10.17148/IJIREEICE.2019.7107

Hardi, S., Sembiring, R., Rachmad, M., Rohana, & Nisja, I. (2022). Simulation of induction motor behavior under voltage sags using alternative transient program. *Journal of Physics: Conference Series*, *2193*(1). https://doi.org/10.1088/1742-6596/2193/1/012030

Mukti, H., Duanaputri, R., Ridzki, I., & Hakim, M. F. (2024). Braking System for a 3-phase Induction Motor in Traditional Petroleum Mining. *International Journal of Electrical Engineering and Applied Sciences (IJEEAS)*, *7*(1). https://doi.org/10.54554/ijeeas.2024.7.01.004

Mukti, H., Duanaputri, R., Sutjipto, R., Hakim, M. F., Hermawan, A., Yusuf, A. T., & Prayoga Rifqi Nanda. (2025). oft Starting of Induction Motors in Traditional Oil Mining Using Arduino Uno. *Proceeding of International Joint Conference on UNESA*, *2*(2).

Patil, P. S., & Porate, K. B. (2009). Starting analysis of induction motor. A computer simulation by etap power station. *2009 2nd International Conference on Emerging Trends in Engineering and Technology, ICETET 2009*, 494–499. https://doi.org/10.1109/ICETET.2009.211

Singarimbun, P., & Anisah, S. (n.d.). *Analysis of Inverter Drive Working System as 3-Phase AC Motor Rotation Speed Regulator*. https://doi.org/10.33258/birex.v4i4.7228

Siregar, Y., Siahaan, Y. R. O., Mohamed, N. N. B., Riawan, D. C., & Yuhendri, M. (2025). Design of starting a three-phase induction motor using direct on-line, variable frequency drive, soft starting, and auto transformer methods. *Indonesian Journal of Electrical Engineering and Computer Science*, *37*(2), 700–714. https://doi.org/10.11591/ijeecs.v37.i2.pp700-714

Suji Prasad, S. J., Suganesh, R., & Suresh Kumar, R. (2019). Safe operation of induction motor with programmable logic controller and human machine interface. *International Journal of Innovative Technology and Exploring Engineering*, *8*(12), 2307–2311. https://doi.org/10.35940/ijitee.L3335.1081219

Taru, A. R., Tupe, B. K., Dalvi, S. R., Ghorpade, A. S., Ladge, A. D., & Sane, S. (n.d.). International Conference on "Role of recent technology in nation-building" A REVIEW ON SPEED CONTROL OF THREE-PHASE INDUCTION MOTOR USING VARIABLE FREQUENCY DRIVE TECHNOLOGY. In *International Engineering Journal For Research & Development* (Vol. 6). www.iejrd.com

Yuhendri, M., Siregar, Y., Candra Riawan, D., Nabila Mohamed, N., Taali, & Hanifah, F. (2025). Vector Control of Three Phase Squirrel Cage Induction Motor based on Internet of Things. *Engineering, Technology and Applied Science Research*, *15*(3), 22312–22318. https://doi.org/10.48084/etasr.9790